International Journal of Cast Metals Research

ISSN: 1364-0461 (Print) 1743-1336 (Online) Journal homepage: https://www.tandfonline.com/loi/ycmr20

Improvement in fracture toughness of austempered ductile iron by two-step austempering process

K. S. Ravishankar, P. P. Rao & K. R. Udupa

To cite this article: K. S. Ravishankar, P. P. Rao & K. R. Udupa (2010) Improvement in fracture toughness of austempered ductile iron by two-step austempering process, International Journal of Cast Metals Research, 23:6, 330-343, DOI: 10.1179/136404610X12693537270091

To link to this article: https://doi.org/10.1179/136404610X12693537270091

Published online: 18 Jul 2013.

Improvement in fracture toughness of austempered ductile iron by two-step austempering process

K. S. Ravishankar, P. P. Rao* and K. R. Udupa

Ductile cast iron samples were austenitised at 900°C and subjected to two types of austempering called as conventional austempering and two-step austempering. Five different temperatures, 280, 300, 320, 350, 380 and 400°C, with an austempering time of 2 h, were chosen for conventional austempering. For two-step austempering process, the first step temperatures were 280, 300 and 320°C. The samples were austempered at each of these temperatures for different times, i.e. 10, 20, 30, 45 and 60 min, and then upquenched to higher temperature of 400°C for 2 h. Fracture toughness and tensile studies were carried out under all these austempering conditions. During conventional austempering, the fracture toughness initially increased with increasing austempering temperature, reached a peak value of 63 MPa $m^{1/2}$ and dropped with further increase in temperature. During the two-step austempering, fracture toughness was found to increase with increasing first step time. The curve shifted to higher values of fracture toughness as the first step temperature was decreased and the maximum value of 78 MPa $m^{1/2}$ was obtained. The results of the fracture toughness study and the fractographic examination were correlated with microstructural features such as bainitic morphology, the volume fraction of retained austenite, and its carbon content. Ferrite lath size and stability of the retained austenite were found to influence the fracture toughness.

Keywords: Austempered ductile Iron, Fracture toughness, Strain induced martensite

Introduction

Austempered ductile iron (ADI) is a very attractive material for many engineering applications because of its excellent combination of high strength and ductility.[1–3] It also exhibits good fatigue resistance and wear properties.[4–8] The remarkable properties of ADI are attributed to its unique microstructure consisting of bainitic ferrite and austenite rather than ferrite and carbide as in austempered steels.[1–3] Because of this difference in microstructure, the product of austempering treatment is referred to as ausferrite rather than bainite. By controlling the austempering temperature and time, the relative proportions of bainitic ferrite and austenite as well as fineness of ferrite can be varied over a wide range. This results in considerable variation in mechanical properties. This wide range of properties offered by austempered ductile iron has made it an attractive material for many engineering applications in automobile industry.[9,10]

Some investigators[11–15] have studied the relationship between microstructure of ADI and its mechanical properties. Now it is fairly well understood that ADI austempered at lower temperatures has high hardness, high strength and low ductility, while that austempered at higher temperatures exhibits lower hardness, lower strength with higher ductility. Thus, it is found that strength decreases with increasing austempering temperature, while the ductility increases simultaneously.

Fracture toughness is a very important parameter for structural design. Because of the importance, many investigators[16–20] have studied the fracture toughness of ADI and found that these are comparable to those of hardened and tempered medium carbon or low alloy steels at similar hardness levels. It is now generally agreed that ADI with lower bainitic microstructure has better fracture toughness than that with upper bainitic microstructure. This leads to the interesting observation that fracture toughness increases with increasing tensile strength.

In a recent investigation, Daber and Rao[21] and Daber *et al.*[22] have shown that a combination of upper and lower bainitic microstructures can be obtained by resorting to two-step austempering, where the ductile iron is austempered at two temperatures rather than at a single temperature as in conventional austempering. It will be interesting to study the effect of such a microstructure on the fracture toughness of ADI.

Department of Metallurgical and Materials Engineering, National Institute of Technology Karnataka, Surathkal, Mangalore, 575025 Karnataka, India

*Correspondence author, email ppr@nitk.ac.in

Received 11 June 2008; accepted 9 February 2009
DOI 10.1179/136404610X12693537270091

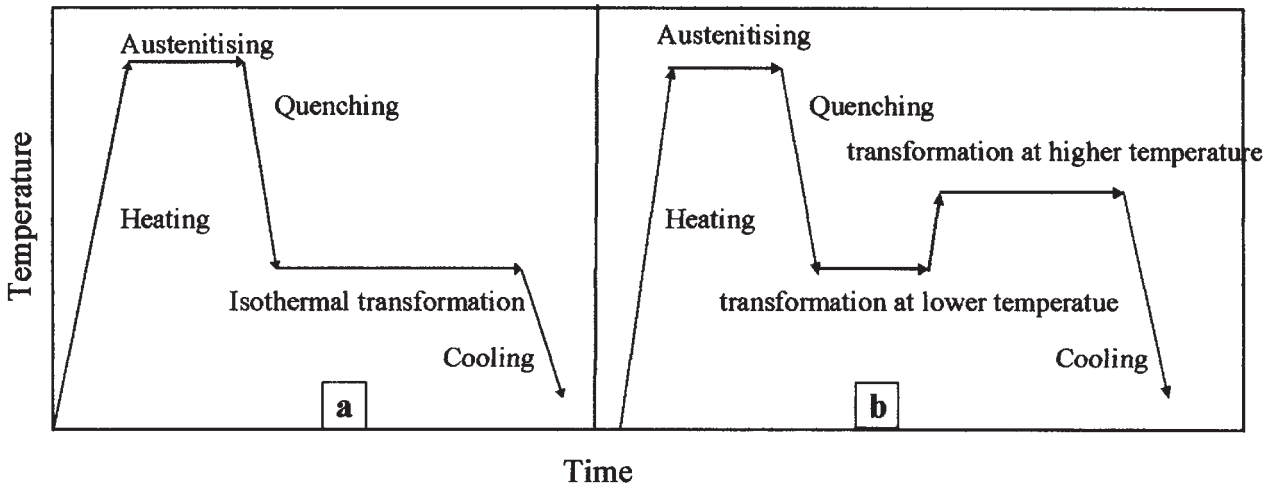

1 Schematic diagram showing *a* conventional and *b* two-step austempering processes

Two-step austempering has been tried by a few investigators. Grech[23] as well as Putatunda and co-workers[24–27] carried out two-step austempering in which the sample was quenched from the austenitising temperature into a salt bath maintained at the lower temperature. After holding for some time at this temperature, the temperature of the salt bath was steadily raised to that of the second step. Bayati *et al.*[28] and Pereloma and Anderson[29] carried out two-step austempering where the first step temperature was higher than that of the second step.

In the present work, the ductile iron samples were initially austempered in a salt bath at a low temperature like 300°C for short durations like 20 min, and then quickly transferred to a second salt bath maintained at the higher temperature of 400°C where it was maintained for 2 h. Unlike in the work of Bayati *et al.*[28] and Pereloma and Anderson,[29] the present work involved austempering at a lower temperature initially followed by that at a higher temperature. Unlike in the works of Grech[23] and those of Putatunda and coworkers,[24–27] both the first and second steps were isothermal treatments. Further, by varying the first step temperature and time, different combinations of microstructures typical of lower and upper austempering temperatures were obtained. Effect of such microstructures on the tensile properties and fracture toughness was investigated.

Experimental work

Material

The chemical composition of the ADI used in the present investigation is reported in Table 1. The material was cast in the form of slabs, $200 \times 150 \times 30$ mm. The nodule count estimated using an image analyser was found to be 100 mm^{-2} with nodularity greater than 90%.

Heat treatment

Two types of austempering heat treatments were carried out, namely, conventional austempering and two-step austempering.

Table 1 Chemical composition of ADI used in present investigation

Element	C	Si	Mn	S	P	Mg	Ni	Mo	Cu
Content, wt-%	3·5	2·8	0·3	0·02	0·02	0·04	1·5	0·3	0·5

In the conventional austempering process, the samples, after austenitising at 900°C for 30 min, were austempered at different temperatures (280, 300, 320, 350, 380 or 400°C) for a fixed austempering time of 2 h. The temperatures were so selected that the first three lower temperatures were expected to produce lower bainitic microstructure, while the three higher temperatures would result in upper bainitic microstructure. Figure 1*a* shows the schematic diagram of the conventional austempering process.

The two-step austempering process consisted of austenitising the sample at 900°C for 30 min followed by austempering at two different temperatures for different durations of time. The first step temperature was 280, 300 or 320°C. After holding the sample at one of these temperatures for different durations of time (10, 20, 30, 45 or 60 min) in a salt bath, it was immediately transferred to another salt bath which was maintained at 400°C. The samples were kept in the second salt bath for a duration of 2 h and then quenched in water. Figure 1*b* shows the schematic diagram of the two-step austempering.

Mechanical testing

Round cylindrical samples of gauge length 36 mm with diameter of 6 mm as shown in Fig. 2*a* were machined

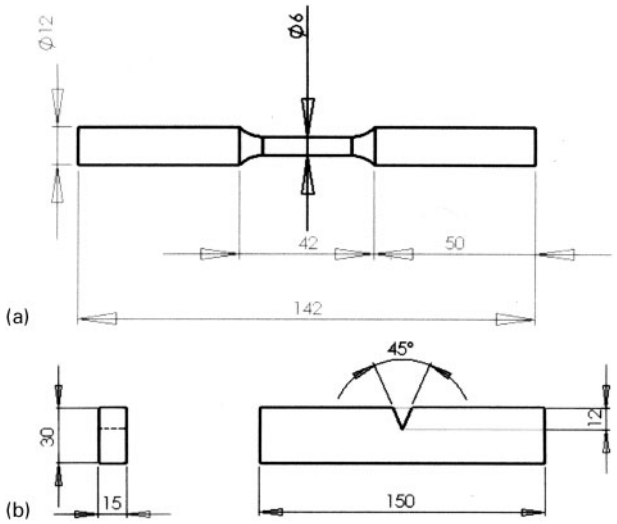

2 Dimensions of *a* tensile and *b* three-point bend specimen in millimetre

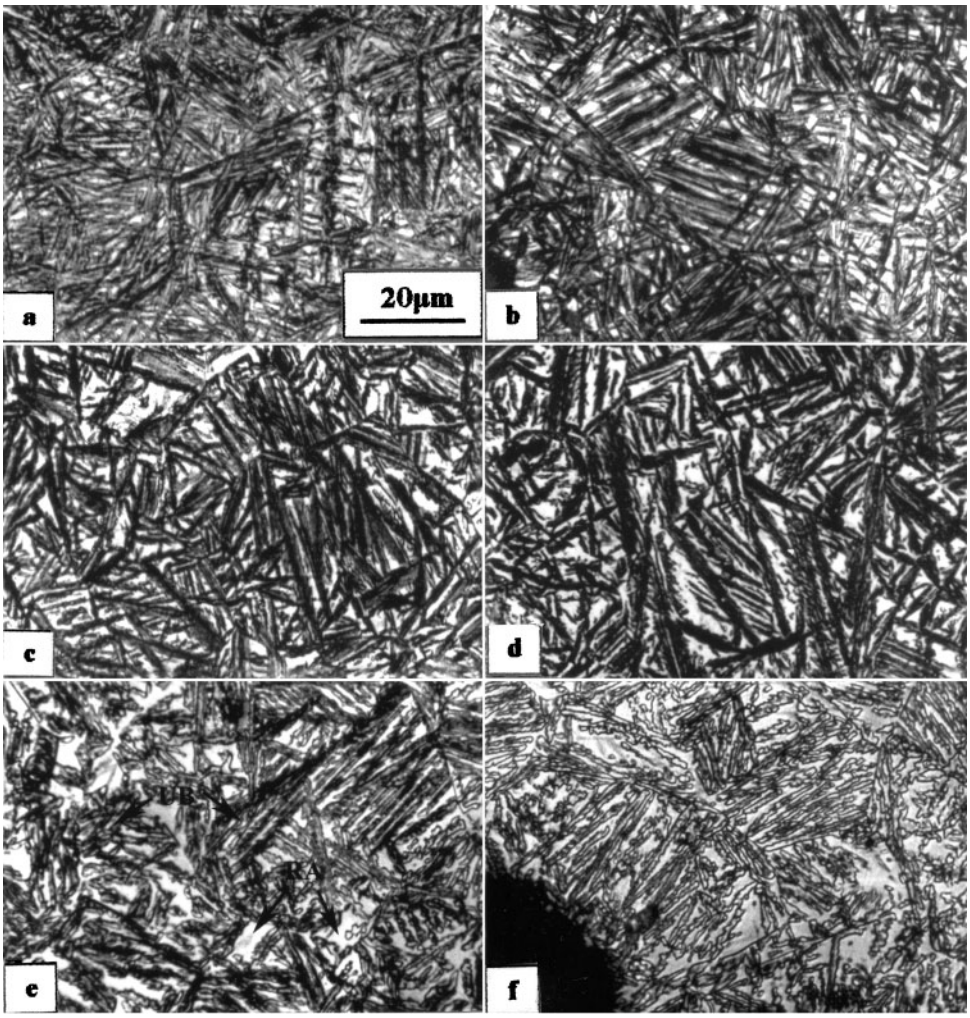

3 Microstructures of samples austempered at *a* 280°C, *b* 300°C, *c* 320°C, *d* 350°C, *e* 380°C and *f* 400°C

for tension test. This test was carried out as per ASTM E8[30] to determine the tensile strength, yield strength and percentage elongation under different austempering conditions. Three samples were tested under each heat treatment condition using an Instron 4206 floor model machine at a constant crosshead speed of 1 mm min^{-1}. The results reported are the average of the three tests.

Three-point bend specimens of dimensions shown in Fig. 2*b* were prepared for fracture toughness testing. The samples were then subjected to the above said heat treatments. Three samples were tested under each heat treatment condition. The fracture toughness values reported are the average of the three tests. First of all, a sharp crack front was produced by the application of cyclically applied load in a precracking machine. The stress intensity factor ΔK was 20 MPa $m^{1/2}$ with a stress ratio of 0·1. The propagation of the crack on both sides of the specimen during cyclic loading was carefully observed using a travelling microscope (accuracy: 0·1 mm) at a magnification of $\times 10$. After the desired crack length was produced, the samples were tested on a servohydraulic computer controlled Instron machine as per ASTM E399[31] at a constant crosshead speed of 1 mm min^{-1}. The graph of load against COD obtained were then analysed to get K_Q. All the validity conditions were then checked to confirm that $K_Q = K_{IC}$.

Fractography

The fracture surfaces of the fracture toughness and tensile samples under all the heat treatment conditions were examined on a Hitachi S-2400 scanning electron microscope to elicit information about the fracture mode.

Metallography

The metallographic studies were carried out under all the heat treatment conditions before and after fracturing of the samples. For the purpose of microstructural characterisation before fracture, dummy samples were subjected to each of the above heat treatment processes together with the machined samples. The metallography on fractured surface was carried out to examine any microstructural changes during deformation. For this purpose, a 2 mm thick sample was cut from the fracture end. After polishing, the samples were etched with 2% nital and examined using optical microscopy under different magnifications to get the information about the morphology of bainitic ferrite and retained austenite and their distribution in the matrix. While preparing the samples of the fracture end for metallographic study, care was taken to retain the microstructure of the deformed layer on the surface of the specimen. The specimens were polished with fine emery papers to get a flat surface. Metallographic studies were also carried out to study the microstructural changes if any around a propagating crack. For this, the samples were loaded

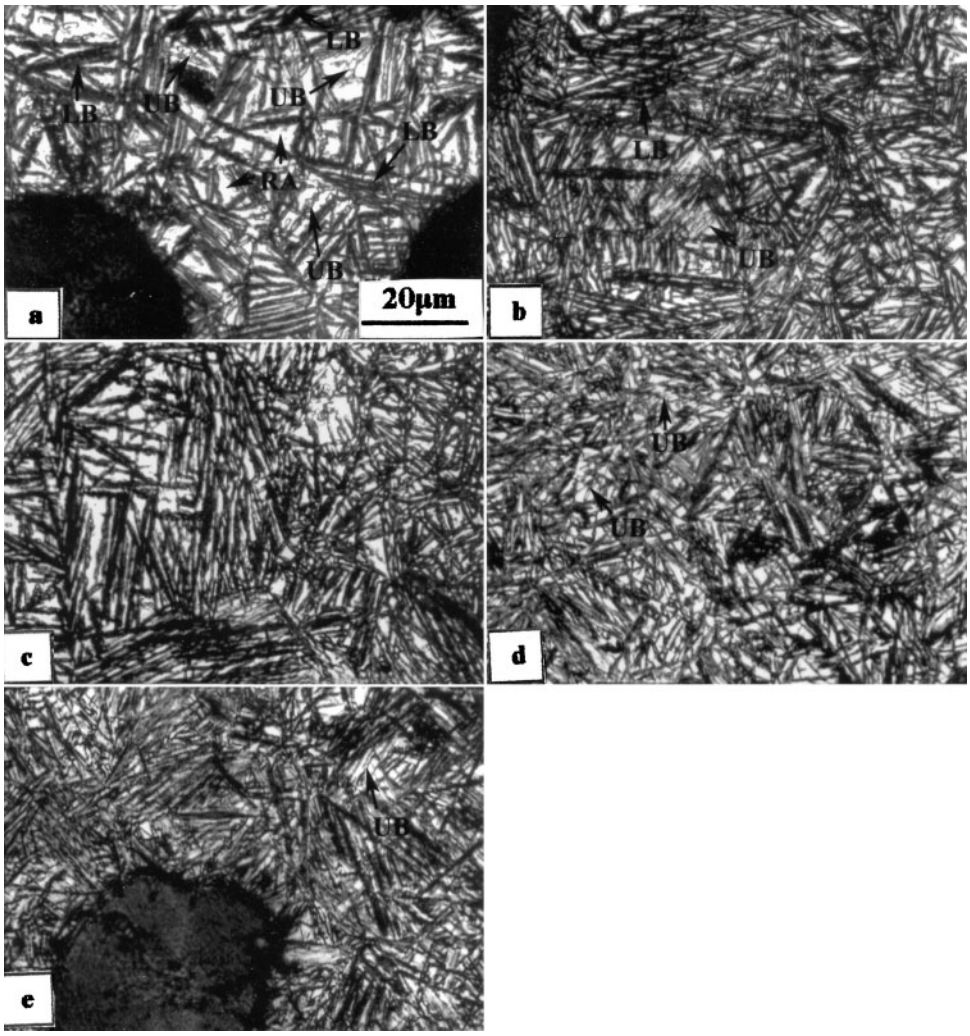

4 Microstructures of samples subjected to two-step austempering with first step temperature of 280°C and first step times of *a* 10 min, *b* 20 min, *c* 30 min, *d* 45 min and *e* 60 min

partly to allow the crack to propagate some distance, but not sufficient to cause complete fracture. A section was taken through the sample to reveal the microstructure at the crack tip as well as along the two flanks.

Microstructural studies were carried out using Jeol analytical scanning electron (model 6380 LA) microscope at magnifications higher than $\times 1000$ to reveal features which could not be seen clearly under the optical microscope.

X-ray diffraction studies were carried out with Cu K_α radiation on Jeol JDX 8P diffractometer at 30 kV and 20 mA. The samples were scanned in the angular 2θ of 40–50° at a scan speed of 0·25° min^{-1}. Direct comparison method of Cullity[32] was used to determine volume fraction of retained austenite and bainitic ferrite. Integrated intensities of the (111) peak of austenite and (110) peak of ferrite were obtained by measuring the area under the peaks using a planimeter. The amount of retained austenite was estimated using the following relationship

$$\frac{I_\gamma}{I_\alpha} = \frac{R_\gamma X_\gamma}{R_\alpha X_\alpha} \tag{1}$$

where I_γ and I_α are the integrated intensities of the (111) peak of austenite and the (110) peak of ferrite respectively; X_α is the volume fraction of ferrite and X_γ is the volume fraction of austenite; the constants R_α and R_γ are given by the following expression for each peak

$$R = \frac{1}{V^2}(Fp\text{LP})e^{-2\text{m}} \tag{2}$$

where V is the atomic volume of unit cell, F is the structure factor; p is the multiplicity factor; LP is the Lorentz polarisation factor and $e^{-2\text{m}}$ is the temperature factor. The carbon content of the retained austenite was estimated using the following relationship[33]

$$a_\gamma = 0{\cdot}3548 + 0{\cdot}0044C_\gamma \tag{3}$$

where a_γ is the lattice parameter of austenite and C_γ is the carbon content of the retained austenite (wt-%).

Results and discussion

Microstructure

Metallographic examination of the samples subjected to conventional austempering showed a systematic change in the microstructure as the austempering temperature was increased. At the lowest temperature of 280°C, very fine sheaths of bainitic ferrite were observed, with only a small amount of retained austenite in between, as shown in Fig. 3*a*. As the temperature was increased, ferrite was found to coarsen, and simultaneously, the amount of

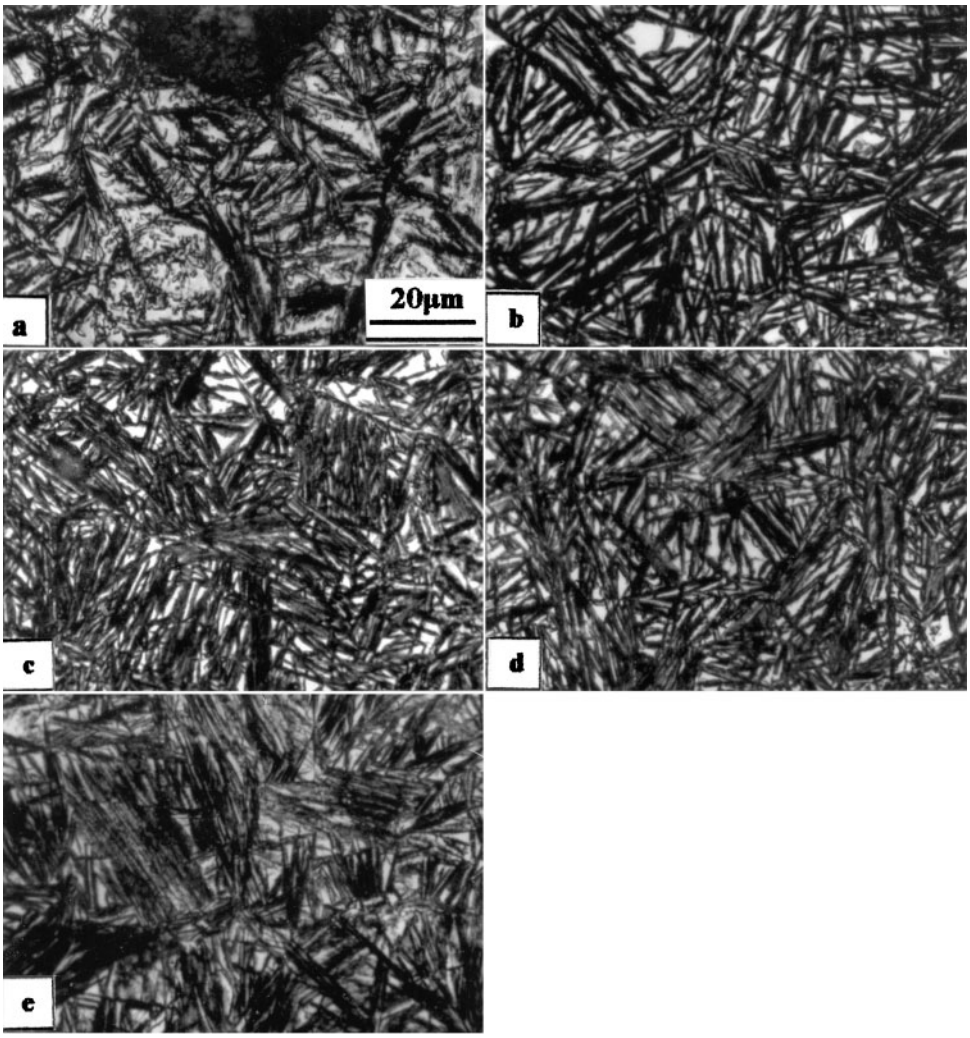

5 Microstructures of samples subjected to two-step austempering with first step temperature of 300°C and first step times of *a* 10 min, *b* 20 min, *c* 30 min, *d* 45 min and *e* 60 min

retained austenite also increased as shown in Fig. 3*b–f*. The morphology of ferrite changed from closely spaced sheaths to isolated broad and coarse laths. The amount of retained austenite increased, particularly at temperatures higher than 350°C. These blocky austenite regions separated well the broad ferrite laths from each other.

In the samples subjected to two-step austempering, the microstructure changed significantly as the first step time was increased. These are shown in Figs. 4–6, for the three first step temperatures, 280, 300 and 320°C respectively. At the short first step time (10 min), little amount of lower bainite was found to coexist with upper bainite, as shown in Figs. 4*a*, 5*a* and 6*a*. The transformation of austenite started with the formation of lower bainite characteristic of the first step temperature. Because of the short duration at this temperature, there would be a significant amount of untransformed austenite when the sample was transferred to the second salt bath at the higher temperature. This would now transform to bainite with a morphology characteristic of the higher temperature. The proportion of this second constituent decreased significantly as the first step time was increased since more lower bainite formed and less untransformed austenite would be available for the second step. At the longest first step time (60 min), the microstructure was seen to be predominantly lower bainite.

While the optical microscopy gave a qualitative picture of the microstructural evolution, quantitative information was obtained through the X-ray diffraction technique. During conventional austempering, the retained austenite content increased from 23 vol.-% at 280°C to 42 vol.-% at 400°C as shown in Fig. 7*a*. This can be explained on the same lines as carried out by previous investigators,[11–15] namely, high nucleation rate of bainitic ferrite and low diffusion rate of carbon in austenite at low temperatures, and low nucleation rate and high diffusion rate at higher temperatures. During the two-step austempering, the retained austenite content decreased from $\sim$40 vol.-% to $\sim$18 vol.-% when the first step time was increased from 10 to 60 min as shown in Fig. 7*b*. As the first step temperature was increased, the curve shifted to higher values of retained austenite.

Through optical microscopy, it was observed that the morphology of ferrite changed considerably with heat treatment conditions. Quantitative data for this were obtained through X-ray diffraction by analysing the (110) peak of ferrite using Scherrer formula:[34]

$$t = 0{\cdot}9\lambda / B\cos\theta \quad (4)$$

where t is the width of ferrite, λ is the wavelength of X-ray, B is the breadth of ferrite peak at half height in

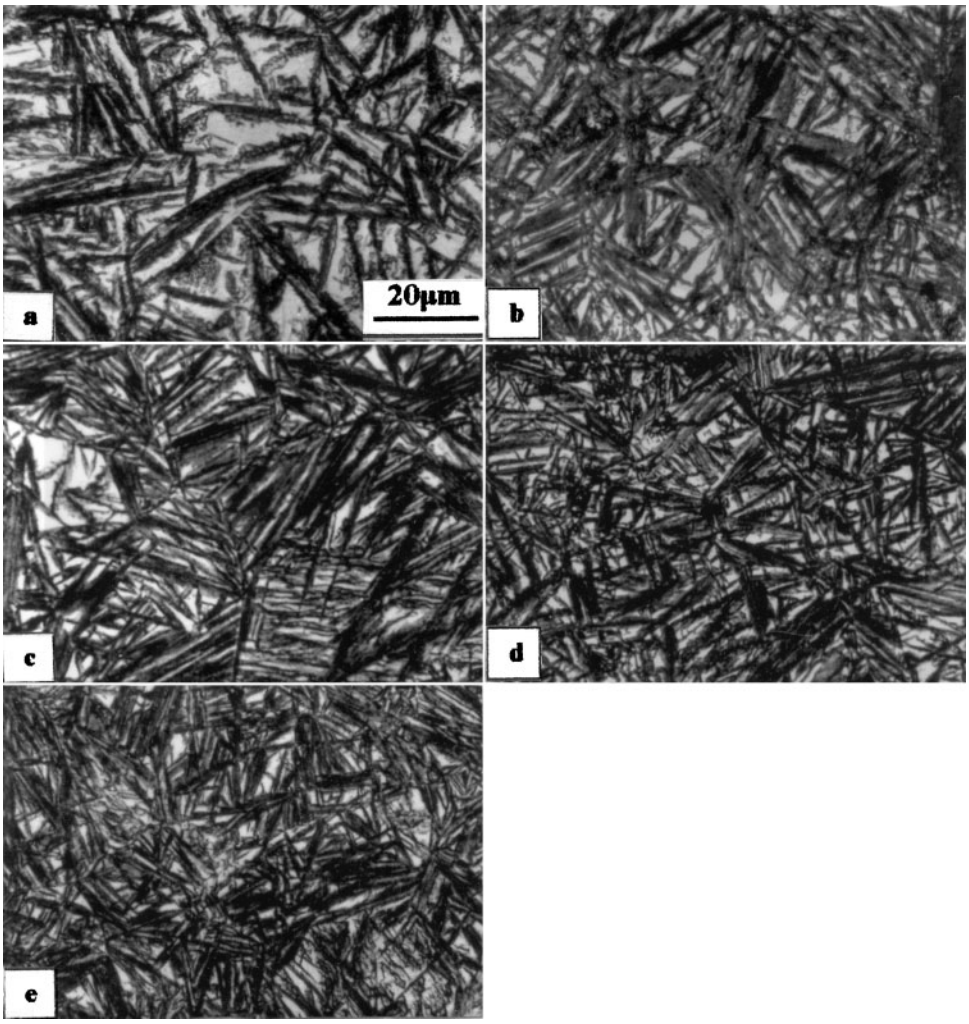

6 Microstructures of samples subjected to two-step austempering with first step temperature of 320°C and first step times of *a* 10 min, *b* 20 min, *c* 30 min, *d* 45 min and *e* 60 min

radians and θ is the Bragg angle. Tables 2 and 3 show the widths of the ferrite resulting from conventional and two-step austempering respectively. These show that the width of ferrite increased with increasing temperature in the case of conventional austempering and decreased with increasing first step time in the case of two-step austempering.

Another important microstructural feature estimated from X-ray diffraction profile was the carbon content of the retained austenite. Figure 8 shows the carbon content of retained austenite during the conventional and two-step austempering processes respectively. During conventional austempering, the carbon content increased from 1·76 wt-% at 280°C to a peak value of 1·82 wt-% at 300°C and decreased thereafter with further increase in temperature, reaching a low value of 1·62 wt-% at 400°C. But in the case of two-step austempering, the carbon content of the retained austenite increased with increasing first step time at a given first step temperature.

At the first step temperature of 300°C, the carbon content increased from 1·68 to 1·94 wt-% when the first step time was increased from 10 to 60 min. This signifies an increase of 5·4% in carbon content of the retained austenite as compared to that in conventional austempering at 300°C for 2 h, which was only 1·84 wt-%. Similar observations could be made at the other two first step temperatures of 280 and 320°C with the first step time of 60 min. In each of these cases, carbon content of the retained austenite was higher as compared to conventional austempering for 2 h at a temperature corresponding to that of the first step of the two-step austempering at a similar fine acicular microstructure.

In addition to the above microstructural features, one more factor to be considered at this stage is the total carbon content of the retained austenite. As already explained earlier, during the bainitic reaction, carbon diffuses from the ferrite regions into the surrounding austenite. Assuming that the microstructure consists of only ferrite and austenite, the matrix carbon content can be estimated as $X_\alpha C_\alpha + X_\gamma C_\gamma$, where X_γ and X_α are the volume fractions of austenite and ferrites respectively, while C_γ and C_α are their respective carbon contents. Taking the carbon content of ferrite as practically zero, the matrix carbon can be represented by $X_\gamma C_\gamma$. Figure 9 shows the total carbon content after the conventional and two-step austempering respectively. In both cases, the maximum value $X_\gamma C_\gamma$ is C_γ^o which is the initial carbon content of the austenite at the given austenitising temperature. The following empirical relationship can be used to estimate C_γ^o[35]

$$C_\gamma^o = T_\gamma/420 - 0{\cdot}17\mathrm{Si} - 0{\cdot}95 \quad (5)$$

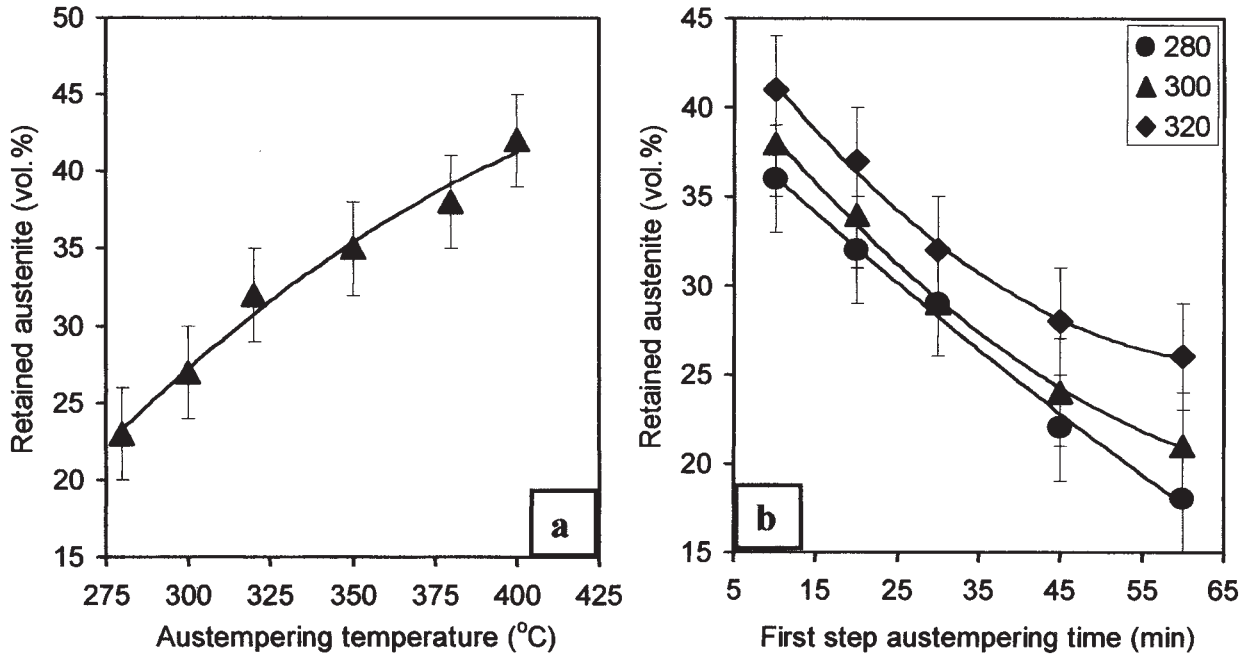

7 Retained austenite after *a* conventional austempering and *b* two-step austempering at first step temperatures indicated on figure

where T_γ is the austenitising temperature (°C) and Si is the silicon content (wt-%). In the present investigation, the austenitising temperature was 900°C and the silicon content was 2·8 wt-%. This gives a value of 0·7 wt-% for C_γ^o. Out of this, the carbon present in the retained austenite can be taken as $X_\gamma C_\gamma$. During conventional austempering, for the samples austempered at 280°C, this is only 0·39 wt-%. The remaining 0·31 wt-% carbon is trapped in ferrite. Part of this may precipitate as carbides within the ferrite, while the rest may be present in the solid solution in ferrite. As the austempering temperature was increased, $X_\gamma C_\gamma$ increased and at 400°C, it was found to be 0·68 wt-%, very close to the original value of C_γ^o of 0·7 wt-%. This can be attributed to the increasing diffusion of carbon into the surrounding austenite at the increasing austempering temperature. Build-up of the carbon ahead of the ferrite hinders its growth and stabilises the austenite, resulting in a large volume fraction of retained austenite. Also, at higher temperatures, the entire carbon is within the retained austenite because of the faster diffusion of carbon from the growing ferrite into the austenite. In the two-step austempering, the maximum in $X_\gamma C_\gamma$ was observed at the lowest first step time of 10 min. This is not surprising since the major transformation took place at 400°C, as the transformation at the first step temperature was only for 10 min. With increasing first step time, the extent of transformation at this temperature increased. At the longest first step time of 60 min, the transformation almost reached the completion stage. In such a case, the amount of retained austenite will be small for the reason explained earlier. Austempering further at 400°C for 2 h does not make any difference. Even though the carbon content for such austempering condition is high, the reduced austenite content will still result in low values of $X_\gamma C_\gamma$.

Table 2 Widths of ferrite sheath after conventional austempering process

Austempering temperature, °C	280	300	320	350	380	400
Width *t*, μm	0·1	0·14	0·16	0·45	0·8	1·2

Mechanical properties

Tensile properties

The results of tensile test are presented in Fig. 10*a* and *b* for conventional and two-step austempering respectively. These figures indicate that lower bainitic microstructure will result in higher yield strength. As shown in Fig. 10*a*, during conventional austempering, the yield strength decreased with increasing austempering temperature. In the two-step austempering process, higher values of yield strengths were obtained for longer first step austempering times. It has been generally concluded that increase in strength with changing austempering conditions is due to the refinement of the microstructure. Hayrynen *et al.*[36] found that the yield strength shows a Hall–Petch type of dependence on ferrite lath size. They concluded that the influence of austenite was negligible and could be ignored. The present results are in agreement with these conclusions as can be seen by comparing the tensile data with ferrite sheath size presented in Tables 2 and 3.

Fracture toughness

The variation in fracture toughness resulting from conventional and two-step austempering processes are shown in Fig. 11. In the case of conventional

Table 3 Widths of ferrite sheath after two-step austempering process

First step austempering temperature, °C	First step austempering time, min				
	10	20	30	45	60
	Width *t*, μm				
280	1·12	0·74	0·58	0·16	0·15
300	1·15	0·80	0·62	0·20	0·18
320	1·18	0·96	0·68	0·24	0·23

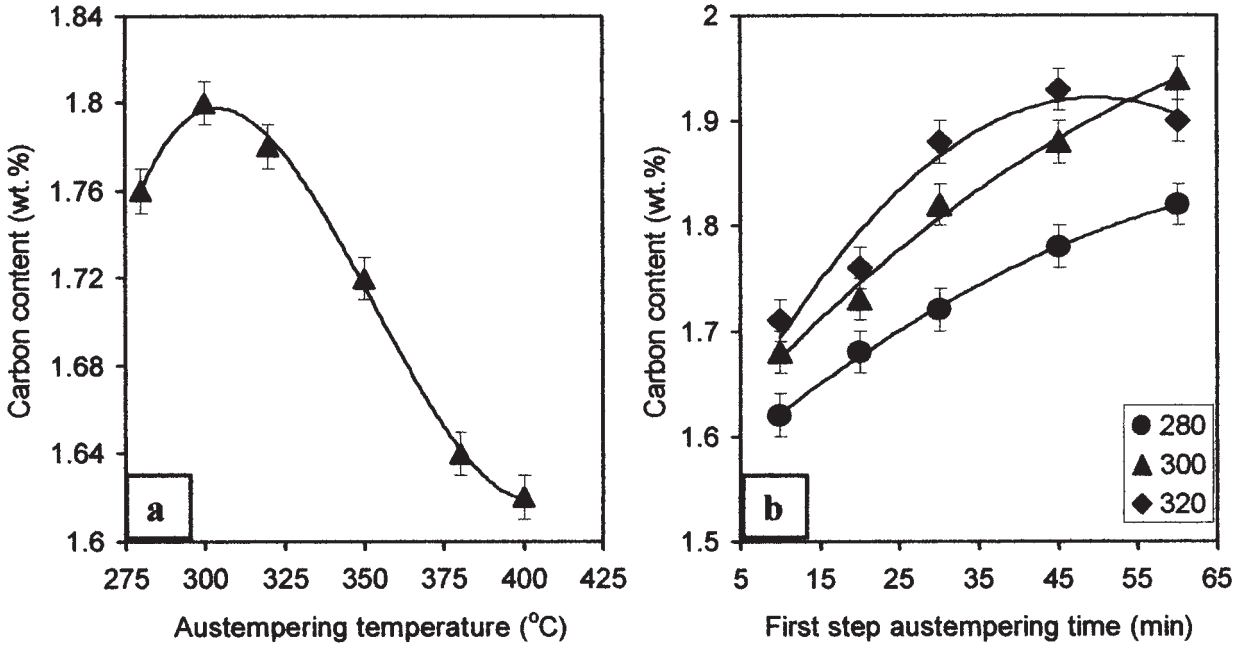

8 Carbon contents of retained austenite after *a* conventional austempering and *b* two-step austempering at first step temperatures indicated on figure

austempering, the fracture toughness initially increased with increasing temperature, reached a peak and then dropped with further rise in temperature. In the case of two-step austempering, the fracture toughness increased with increasing first step time. This was true at all the three first step temperatures employed in the present investigation.

During loading, the plastic deformation is expected to be primarily concentrated within the ferrite laths, which is the weaker of the two constituents. Continued deformation will lead to crack initiation within the ferrite lath or at the ferrite/austenite interface due to dislocation pile ups. Such cracks may form at several locations, and eventually join up to reach critical length causing complete fracture of the material. The smaller the ferrite lath size, the higher the stress required to initiate the microcrack as the dislocation pile-ups at the ferrite/austenite interface will be small. Fracture toughness will therefore increase with decreasing ferrite lath size. It should be noted that the finer the ferrite lath size, the higher the strength. The authors therefore have the interesting phenomenon of increasing fracture toughness with increasing tensile strength, as can be seen from Fig. 10*a* and *b*.

Apart from the ferrite lath size, the stability of the retained austenite is another factor which will have a major effect on the fracture toughness of ADI. The stability of the austenite depends on several factors such

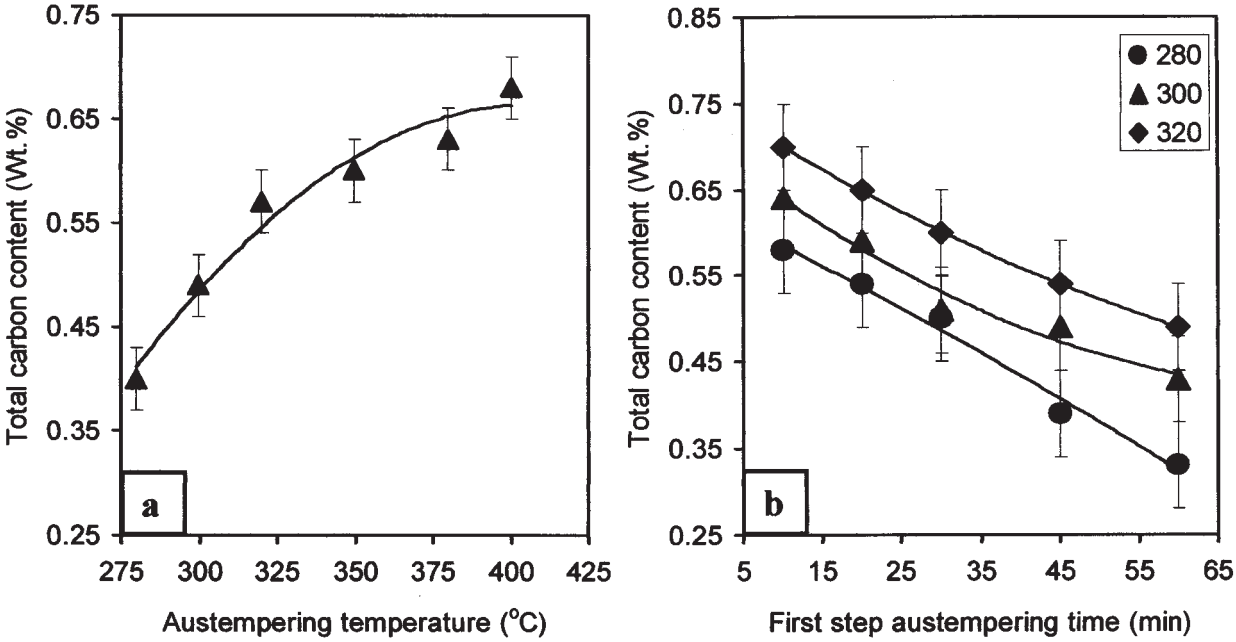

9 Total carbon content after *a* conventional austempering and *b* two-step austempering at first step temperatures indicated on figure

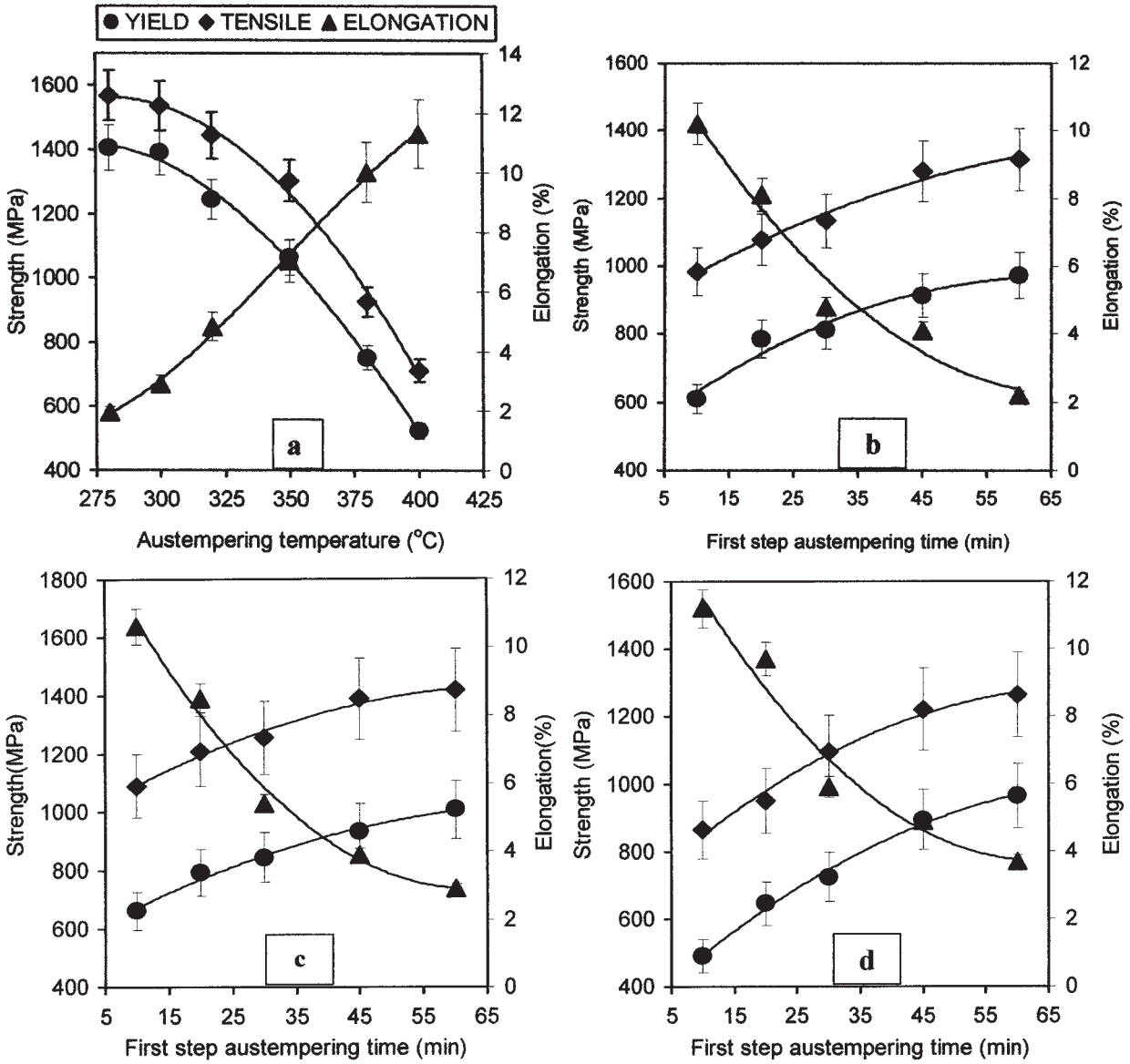

10 Tensile properties after *a* conventional austempering and *b–d* two-step austempering at first step temperatures of 280, 300 and 320°C respectively.

as carbon content of the austenite, size and morphology of the austenite, and its distribution within the microstructure. Carbon content determines the chemical driving force for the martensite transformation. At low carbon contents, the transformation is easy. The retained austenite transforms quickly to martensite, and not much deformation is suffered by the sample. At the same time, if the carbon content is very high (>1·8 wt-%), the transformation to martensite may never occur due to the high stability of the retained austenite. An intermediate carbon content will give the right degree of stability to the retained austenite. Size of the retained austenite is another important factor.[37] At austenite grain sizes smaller than 10 μm, the interfacial energy required for the formation of martensite needles increases exponentially as the grain size decreases.[38] This increases the driving force necessary for the formation of martensite, thereby increasing the stability of the retained austenite. When the retained austenite is present as thin films, the transformation to martensite is virtually impossible because of the very high driving force necessary. On the other hand, large sized blocky austenite can transform relatively easily at low strain levels. Location of the austenite is also important.[39] Austenite present in the vicinity of martensite can transform more rapidly as the martensite can easily transfer the stress directly to the surrounding austenite. Ferrite in the vicinity of austenite can block the formation of further martensite through autocatalytic effect. In the present investigation, a variety of microstructures were produced through different heat treatments. The microstructures consisted of very thin film of austenite on one extreme and broad blocky austenite on the other extreme. The carbon content also varied considerably.

Hence, microstructural studies were conducted in order to elicit information on the stability of the austenite. The fracture surfaces of tensile as well as fracture toughness samples under different heat treatment conditions were studied by optical microscopy, scanning electron microscopy and X-ray diffraction. It was found that under conventional austempering, samples austempered at 300°C showed no presence of martensite, while those austempered at 400°C showed

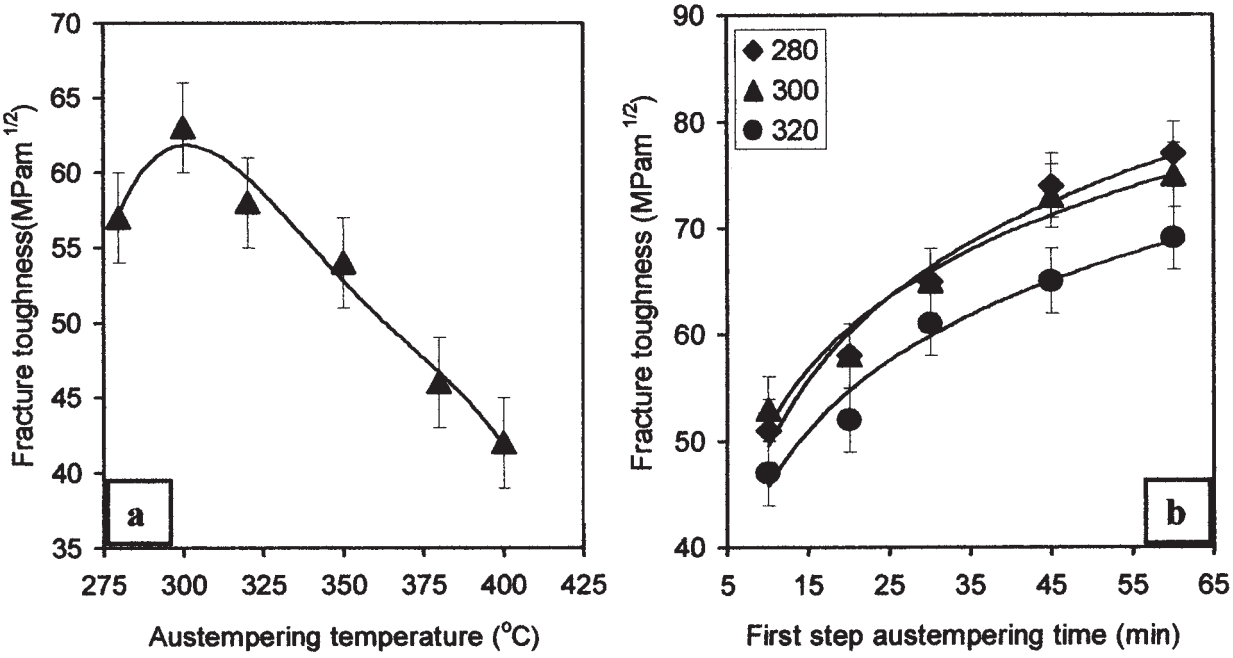

11 Fracture toughnesses after *a* conventional austempering and *b* two-step austempering at first step temperatures indicated on figure

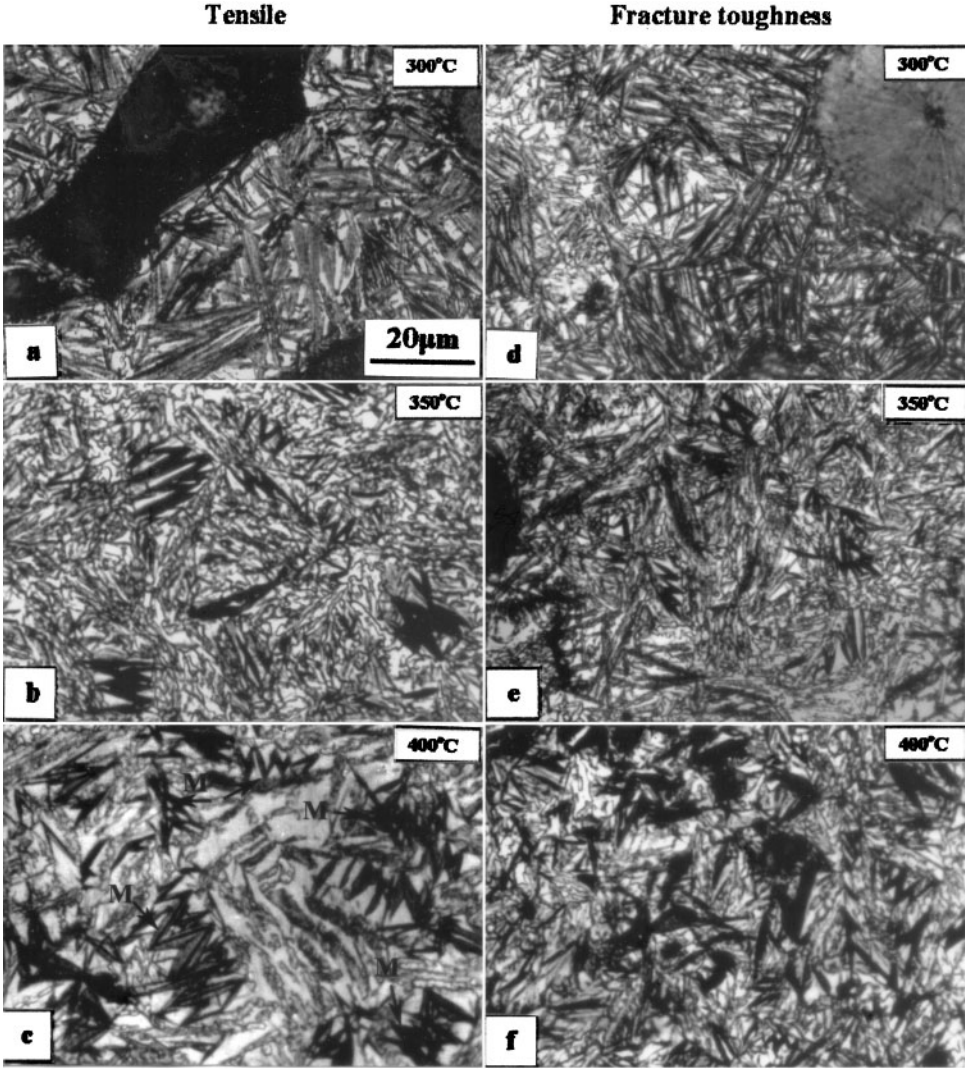

12 Microstructures on fracture surfaces of tensile and fracture toughness samples austempered at temperatures indicated on figure

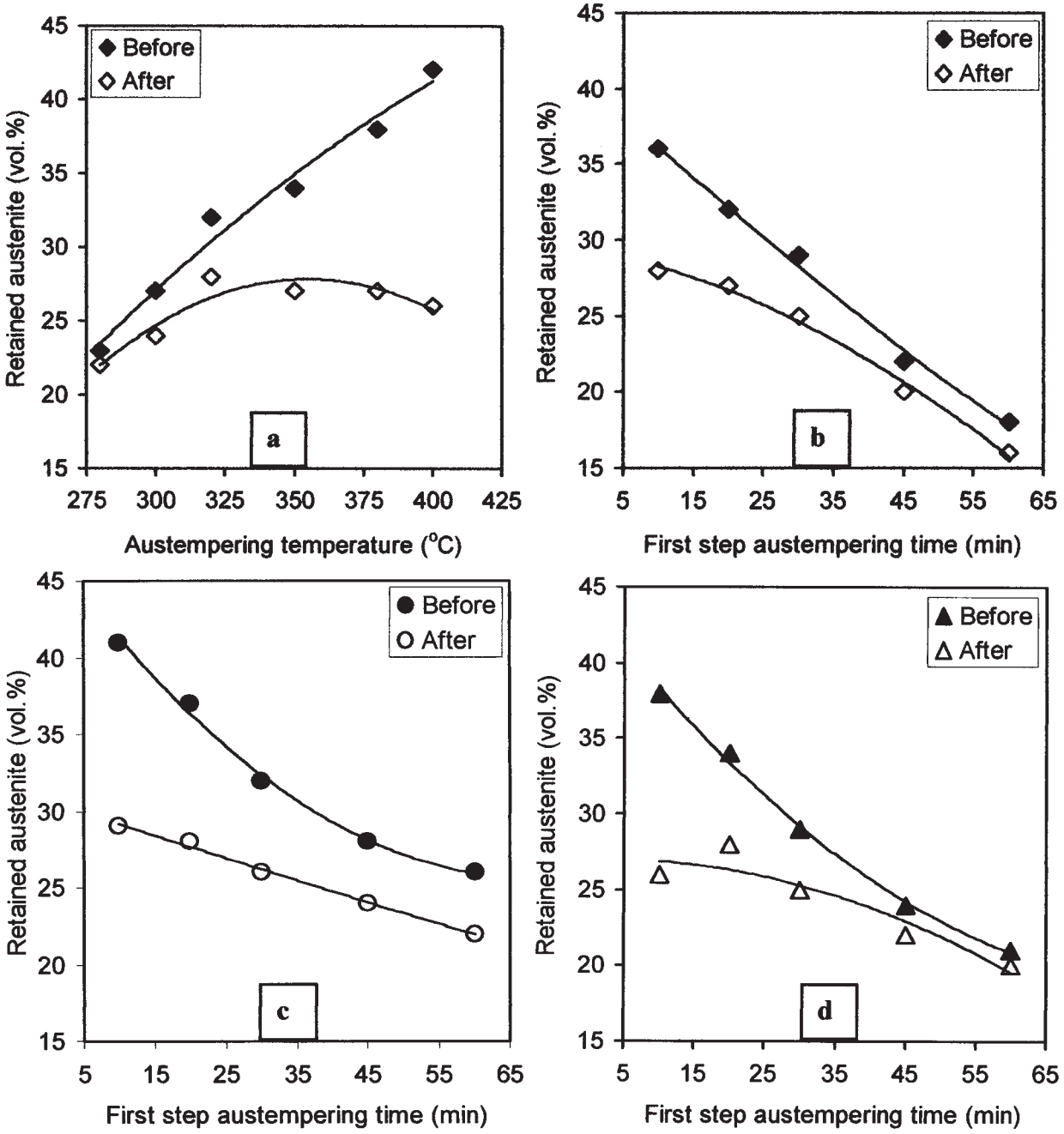

13 Retained austenite contents before and after deformation for *a* conventional austempering and *b–d* two-step austempering at first step temperatures of 280, 300 and 320°C respectively.

copious formation of martensite. The extent of martensite formation increased with increasing austempering temperature. The results are presented in Fig. 12. This is further corroborated by X-ray diffraction results in Fig. 13. These present the retained austenite content on the fracture surfaces of the tensile samples under different heat treatment conditions. The figures also incorporate the retained austenite content in the undeformed samples, which are the same as those of Fig. 7, for the sake of easy comparison. It can be seen that the retained austenite content in the sample subjected to conventional austempering dropped from 43 vol.-% to ~26 vol.-% after fracture, while that austempered at 280°C showed hardly any change. In the case of samples subjected to two-step austempering, the stability was found to increase with increasing first step time as shown in Fig. 13*b–d*. Figure 14*a* shows the microstructure in the vicinity of the crack in a sample austempered at 400°C in which the crack had partly propagated, and the sample had not fully fractured. The microstructure is a section through the sample showing the crack and the regions on either side of the crack. Martensite needles are clearly visible within the retained austenite. The formation of martensite was found to decrease as one moved away from the crack surface, showing clearly the effect of strain. Figure 14*b* shows a region ahead of the crack tip. Once again copious formation of martensite in the immediate vicinity of the crack tip is clearly evident. Figure 15 shows the microstructures near the crack edge and ahead of the crack tip respectively in a sample austempered at 300°C. There was no evidence of martensite formation.

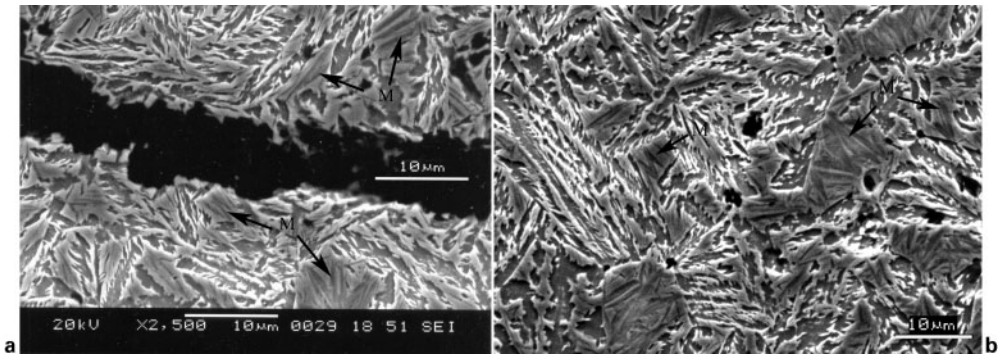

a along crack flanks; *b* ahead of crack tip

14 Microstructure of partly cracked sample austempered at 400°C

The above results indicate that generally, the retained austenite is quite stable in the samples austempered at low temperatures such as 300°C, and was unstable in the samples austempered at high temperatures like 400°C. This can be attributed primarily to the size and morphology of the retained austenite, and to some extent to the carbon content. At low austempering temperatures, the retained austenite was in the form of thin film between sheaths of ferrite. It had relatively high carbon content. On the other hand, at high austempering temperatures, the retained austenite was bulky, large in size, well separated from the ferrite regions, and had relatively low carbon content.

In the case of samples subjected to two-step austempering, copious formation of martensite was noticed in the samples subjected to short first step times. There was hardly any martensite formation in the samples subjected to a longer first step time. The samples austempered for short first step durations like 10 min had a large volume fraction of bulky austenite, and had relatively low carbon content. Hence, the retained austenite was highly unstable. On the other hand, the samples austempered for longer first step times like 60 min had very fine retained austenite in the form of thin films between ferrite sheaths, and had relatively high carbon content. Hence, the retained austenite was highly stable. The stability of the retained austenite is one of the important factors contributing to the improved fracture toughness of the samples subjected to conventional austempering at low temperatures, or long durations of first step austempering in the two-step austempering process.

The formation of the strain induced martensite should have interesting effect on the deformation behaviour since it is the basis of transformation induced plasticity (TRIP) phenomenon. Conventionally, it is believed that TRIP steels should contain lath martensite containing less than 0·2%C, as these will be softer and more ductile than plate martensite. The latter are to be avoided as they are brittle and provide an easy path for crack propagation, which would be detrimental to improved toughness. In ADI, carbon content of the retained austenite is very high. Therefore, plate martensite is expected to form which is hard and brittle. Whether such a transformation will induce plasticity is doubtful. In order to elicit some information on this, fracture surfaces of the fracture toughness and tensile samples subjected to conventional austempering were studied under SEM and the results are presented in Fig. 16. Both fracture toughness and tensile samples austempered at 300°C showed fully dimpled fracture as shown in Fig. 16*a* and *c*, while those austempered at 400°C showed predominantly cleavage type of fracture as shown in Fig. 16*b* and *d*. Thus, in the sample austempered at 400°C, formation of strain induced martensite ahead of the crack tip provides an easy crack path which results in brittle cleavage fracture. This tendency to form strain induced martensite decreases as the austempering temperature is decreased due to the increasing stability of the retained austenite. The fracture mode thus changes from the cleavage type to dimpled one. The formation of martensite does not appear to contribute much to the toughness of ADI containing larger volume fractions of retained austenite. The high tensile elongation of these is more due to the large volume fraction of retained austenite rather than to the formation of martensite during plastic deformation. The detrimental effect of martensite is

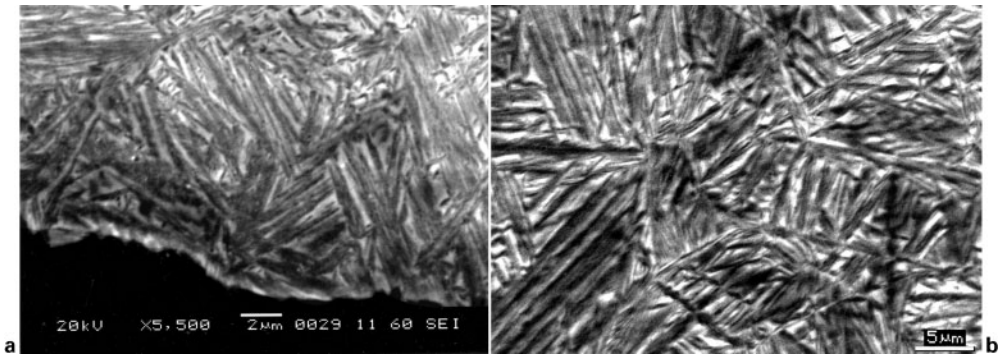

a along crack flanks; *b* ahead of crack tip

15 Microstructure of partly cracked sample austempered at 300°C

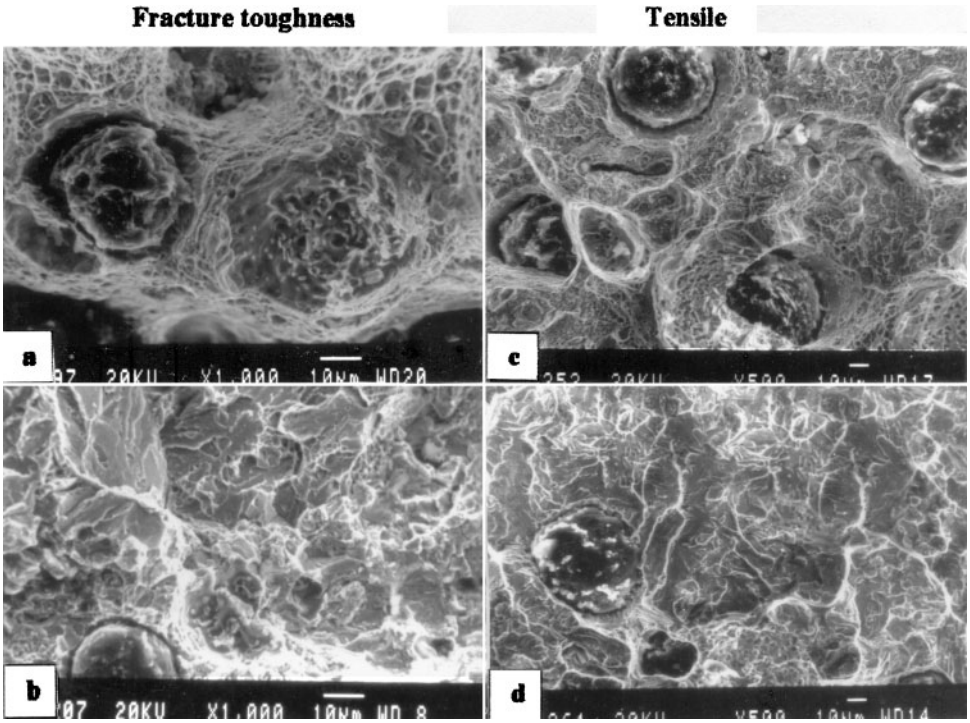

16 Fractographs of fracture toughness and tensile samples. *a* and *c* austempered at 300°C, *b* and *d* austempered at 400°C

accelerated in the fracture toughness test due to the presence of triaxial state of stress at the root of the notch. Notched bar tests in tension or impact are preferred when one determines the tendency of a material to behave in a brittle manner.[40] Testing with a notched sample can bring out differences which cannot be noticed in tension testing. The presence of massive blocky austenite is therefore detrimental to fracture toughness of ADI.

The above discussion clearly indicates that the fracture toughness is attributable to interplay between the effects of ferrite lath size and the stability of austenite. The variation in the microstructure as well as the fracture toughness in both austempering processes followed a similar trend. As explained earlier, though the samples subjected to conventional austempering at lower temperatures exhibited only small amounts of retained austenite, the carbon content was quite high. Similar condition was achieved in two-step austempering by increasing the first step austempering time. The X-ray diffraction profiles showed that, for the two-step austempering, the carbon content of the retained austenite was much higher than that for conventional austempering. This can be attributed to the greater diffusivity of carbon at higher temperature after the sample was held for a predetermined length of time at the lower austempering temperature. It is postulated that the carbon rejected from regions transforming to ferrite is present essentially along ferrite/austenite interface. This will diffuse faster into the austenite at the second step temperature, contributing to improved stability of retained austenite. The process not only refines the microstructure, particularly at longer first step times, but also results in an increased carbon content of the retained austenite. Both these factors lead to an improvement in the fracture toughness as compared to those of conventional austempering. A judicious selection of two-step austempering parameters can result in 20–25% increase in fracture toughness over conventional austempering.

Conclusions

The following conclusions can be drawn from the present investigation:

1. Two-step austempering results in a microstructure which consists of a mixture of fine and coarse ferrite. The relative proportions of these depend on the first step time.
2. The retained austenite content decreases with increasing first step time, while the carbon content of the retained austenite increases.
3. While the tensile and yield strengths increase with increasing first step time, the ductility decreases.
4. The fracture toughness increases with increasing first step time.
5. The best fracture toughness of 78 MPa $m^{1/2}$ obtained through two-step austempering is $\sim$24% higher than that obtained through conventional austempering.
6. The improved fracture toughness resulting from two-step austempering can be attributed to the increased carbon content of the retained austenite and refinement of the microstructure.
7. Strain induced martensite forms during deformation of ADI if the microstructure primarily consists of bulky austenite with low carbon and coarse ferrite.
8. Formation of strain induced martensite is detrimental to fracture toughness as it provides an easy cleavage path for fracture to propagate. This accounts for the observed variation of fracture toughness with austempering temperature during conventional austempering and that with first step time during two-step austempering.

Acknowledgement

This work was financially supported by the Council of Scientific and Industrial Research, New Delhi, India.

References

1. R. B. Gundalach and J. F. Janowak: *Met. Prog.*, 1985, **128**, (2), 19–26.
2. R. B. Gundalach and J. F. Janowak: *AFS Trans.*, 1983, **91**, 3777–3788.
3. G. Wilkinson and C. Grupke: Proc. 2nd Int. Conf. on 'Austempered ductile iron', Ann Arbor, MI, USA, March 1986, ASME Gear Research Institute, 349–358.
4. M. Johansson: *AFS Trans.*, 1977, **85**, 117–122.
5. R. A. Harding: *Met. Mater.*, 1986, **2**, 65.
6. P. Shanmugam, P. P. Rao, K. R. Udupa and N. Venkataraman: *J. Mater. Sci.*, 1994, **29**, 4933–4940.
7. I. Schmidt: *Z. Metalkd*, 1984, **75**, 747–751.
8. S. M. Shah and J. D. Verhoeven: *Wear*, 1986, **113**, 267–273.
9. T. Shiokawa: 'Production experience in austempering of ductile iron castings', Proc. 1st Int. Conf. on ADI, Chicago, IL, USA, ASM, April 1984, 2–4.
10. J. F. Janowak, R. B. Gundlach, G. T. Eldis and K. Rohrig: Proc. 48th Int. Foundry Cong., Varna, Bulgaria, World Foundrymen Organisation, October 1981, 1–15.
11. D. J. Moore, T. N. Rouns and K. B. Rundman: *AFS Trans.*, 1985, **93**, 765–776.
12. T. N. Rouns, K. B. Rundman and D. M. Moore: *AFS Trans.*, 1984, **92**, 815–839.
13. N. Darwish and R. Elliott: *Mater. Sci. Technol.*, 1993, **9**, 586–602.
14. N. Darwish and R. Elliott: *Mater. Sci. Technol.*, 1993, **9**, 882–889.
15. P. P. Rao and S. K. Putatunda: *Metall. Mater. Trans. A*, 1997, **28A**, 1457–1470.
16. I. Bartosiewricz, I. Singh, F. A. Alberts, A. R. Krause and S. K. Putatunda: *J. Mater. Eng. Perform.*, 1993, **4**, 90–101.
17. S. K. Putatunda and I. Singh: *J. Test. Eval.*, 1995, **23**, 325–332.
18. S. K. Putatunda, R. Gupta and P. P. Rao: *Microstruct. Sci.*, 1996, **24**, 103–110.
19. P. P. Rao and S. K. Putatunda: *Metall. Mater. Trans. A*, 1998, **29A**, 3005–3015.
20. P. P. Rao and S. K. Putatunda: *Mater. Sci. Technol.*, 1998, **14**, 1257–1265.
21. S. Daber and P. P. Rao: *J. Mater. Sci.*, 2008, **43**, 357–367
22. S. Daber, K. S. Ravishankar and P. P. Rao: *J. Mater. Sci.*, 2008, **43**, 4929–4937.
23. M. Grech: Proc. World Conf. on 'Austempered ductile iron', Bloomingdale, IL, USA, March 1991, AFS, 600–621.
24. S. K. Putatunda: *Mater. Sci. Eng. A*, 2001, **A315**, 70–80.
25. J. Yang and S. K. Putatunda: *Mater. Sci. Forum*, 2003, **913**, 913–918.
26. J. Yang and S. K. Putatunda: *Mater. Sci. Eng. A*, 2005, **A393**, 254–268.
27. S. K. Putatunda: *Mater. Des.*, 2004, **25**, 219–230.
28. H. Bayati, R. Elliot and G. W. Lorimer: *Mater. Sci. Technol.*, 1995, **11**, 776–786.
29. E. V. Pereloma and C. S. Anderson: *Mater. Sci. Technol.*, 2006, **22**, 1112–1118
30. ASTM International: 'Annual book of ASTM standards', 03·01, 745; 1992, Philadelphia, PA, ASTM International.
31. ASTM International: 'Annual book of ASTM standards', 03·01, 130; 1992, Philadelphia, PA, ASTM International.
32. B. D. Cullity: 'Elements of X-ray diffraction', 411; 1974, Reading, MA, Addison-Wesley.
33. C. S. Roberts: *Trans. AIME*, 1953, **197**, 203–204.
34. B. D. Culity: 'Elements of X-ray diffraction', 102; 1974, Reading, MA, Addison-Wesley.
35. R. C. Voigt and C. R. Loper: Proc. 1st Int. Conf. on 'Austempered ductile iron', 83; 1984, Metals Park, OH, ASM International.
36. K. L. Hayrynen, D. J. Moore and K. B. Rundman: *AFS Trans.*, 1992, **98**, 471–476.
37. M. Takahashi and H. K. D. H. Bhadeshia: *Mater. Trans., JIM*, 1991, **3**, 689–696.
38. J. Wang and S. van der Zwaag: *Metall. Mater. Trans. A*, 2001, **32A**, 1527–1539.
39. I. Tsukatani, S. Hashimoto and T. Inoue: *ISIJ Int.*, 1991, **31**, (9), 992–1000.
40. G. E. Dieter: 'Mechanical metallurgy', 371; 1961, New York, McGraw-Hill Book Company.